Author(s): Nasibulin, Albert G & Shandakov, Sergey D & Nasibulina, Larisa I & Cwirzen, Andrzej & Mudimela, Prasantha R & Habermehl-Cwirzen, Karin & Grishin, Dmitrii A & Gavrilov, Yuriy V & Malm, Jari E M & Tapper, Unto & Tian, Ying & Penttala, Vesa & Karppinen, Maarit & Kauppinen, Esko I

Title: A novel cement-based hybrid material

Year: 2009

Version: Final published version

A novel cement-based hybrid material

Albert G Nasibulin[1,8]**, Sergey D Shandakov**[1,2]**,
Larisa I Nasibulina**[1]**, Andrzej Cwirzen**[3]**, Prasantha R Mudimela**[1]**,
Karin Habermehl-Cwirzen**[3]**, Dmitrii A Grishin**[4]**, Yuriy V Gavrilov**[4]**,
Jari E M Malm**[5]**, Unto Tapper**[6]**, Ying Tian**[1]**, Vesa Penttala**[3]**,
Maarit J Karppinen**[5] **and Esko I Kauppinen**[1,7,8]

[1] Department of Applied Physics and Center for New Materials,
Helsinki University of Technology, Espoo, PO Box 5100, FIN-02150, Finland
[2] Laboratory of Carbon NanoMaterials, Department of Physics,
Kemerovo State University, Kemerovo 650043, Russia
[3] Laboratory of Building Materials Technology, Faculty of Engineering
and Architecture, Helsinki University of Technology, Espoo, PO Box 5100,
FIN-02150, Finland
[4] Mendeleev University of Chemical Technology, Miusskaya pl. 9, Moscow,
125190, Russia
[5] Laboratory of Inorganic Chemistry, Department of Chemistry, Helsinki
University of Technology, Espoo, PO Box 6100, FIN-02150, Finland
[6] Fine Particles, VTT Technical Research Centre of Finland, Biologinkuja 7,
Espoo, PO Box 1000, 02044 VTT, Finland
[7] VTT Biotechnology, Biologinkuja 7, 02044, Espoo, Finland
E-mail: albert.nasibulin@tkk.fi and esko.kauppinen@tkk.fi

Abstract. Carbon nanotubes (CNTs) and carbon nanofibers (CNFs) are known to possess exceptional tensile strength, elastic modulus and electrical and thermal conductivity. They are promising candidates for the next-generation high-performance structural and multi-functional composite materials. However, one of the largest obstacles to creating strong, electrically or thermally conductive CNT/CNF composites is the difficulty of getting a good dispersion of the carbon nanomaterials in a matrix. Typically, time-consuming steps of purification and functionalization of the carbon nanomaterial are required. We propose a new approach to grow CNTs/CNFs directly on the surface of matrix particles.

[8] Author to whom any correspondence should be addressed.

IOP Institute of Physics ⬥ DEUTSCHE PHYSIKALISCHE GESELLSCHAFT

As the matrix we selected cement, the most important construction material. We synthesized in a simple one-step process a novel cement hybrid material (CHM), wherein CNTs and CNFs are attached to the cement particles. The CHM has been proven to increase 2 times the compressive strength and 40 times the electrical conductivity of the hardened paste, i.e. concrete without sand.

Contents

1. Introduction

Carbon nanomaterials, such as carbon nanotubes (CNTs) and carbon nanofibers (CNFs), have recently received tremendous scientific interest due to their remarkable and useful properties, such as exceptional tensile strength, elastic modulus and electrical and thermal conductivity [1, 2]. These materials are promising candidates for the next-generation high-performance structural and multi-functional composite materials [3]–[5].

One of the largest obstacles to creating strong, electrically or thermally conductive CNT/CNF composites is the difficulty of obtaining a good dispersion of the carbon nanomaterials in a matrix. Typically, time-consuming steps of carbon nanomaterial purification, functionalization and mixing with matrix are required. Here we propose a new simple approach to grow CNTs/CNFs directly on the surface of matrix particles. As an example of the matrix we selected cement, one of the most important construction materials. Therefore, the produced carbon nanomaterials are homogeneously dispersed in the matrix and intermingled with the products during the hydration process as shown in figure 1. Thereby, we synthesized a novel cement hybrid material (CHM), wherein CNTs and CNFs are attached to the cement particles, providing an exceptional dispersion of the carbon nanomaterial in the matrix. CHM has been proven to increase 2 times the compressive strength and 40 times the electrical conductivity of the hardened paste, i.e. concrete without sand.

2. Experimental details

2.1. Synthesis

The synthesis of CHM was carried out in a simple one-step process by the chemical vapour deposition (CVD) method considered to be the most viable and efficient process for high-yield CNT production. As the main disadvantage of the CVD method [6]–[14] is the discontinuity of the synthesis processes: catalyst should be separately prepared (usually by wet chemistry), calcinated, reduced and only after that used for the growth of CNTs, we developed a CVD

Table 1. Oxide component content (wt.%) of the Portland cements utilized for CNT/CNF growth.

Cement type	Oxides							
	CaO	SiO_2	SO_3	Fe_2O_3	Al_2O_3	MgO	K_2O	Na_2O
SR cement	63.1	20.2	3.00	4.0	2.2	2.0	0.31	0.48
White cement	68.7	25.2	2.17	0.33	2.1	0.56	0.06	0.18

reactor enabling continuous feeding of the catalyst particles (figure 1). Since cement particles naturally contain both catalyst and inert support substances required for the CVD synthesis, we have utilized for the first time this inexpensive basic building material for CNT and CNF fabrication. This allowed us to avoid the many time-consuming steps of catalyst-support preparation. We have examined two types of Portland cement with different concentrations of iron oxide (Fe_2O_3): sulphate-resistant (SR) (4 wt%) and white (0.33 wt%) Portland cements (table 1). It is worth noting that SiO_2, MgO and Al_2O_3 are known to be good supporting materials for the growth of CNTs [15]–[17]. For the syntheses, acetylene was chosen as the main carbon source due to its low decomposition temperature and cost effectiveness. As promoting additives in order to enhance the yield, we examined carbon monoxide and carbon dioxide.

The synthesis of CHM was carried out in a CVD reactor, which consists of a quartz tube (with an internal diameter of 34 mm and a length of 100 cm) inserted in a resistively heated furnace (with a heated length of 60 cm), a powder feeder with an adjustable powder feeding rate, a copper screw feeder, a powder collector and a water cooling system to keep the ends of the tube at room temperature (figure 1). The residence time of the cement particles in the high-temperature reactor zone (about 30 cm) was regulated by the motor rotation speed, which was varied from 1 to 6 min^{-1} corresponding to 30 and 5 min, respectively. All the reported results were typically obtained at 4 min^{-1}, unless otherwise specified. The experimental investigations were carried out with a powder feeding rate of 30 g h^{-1} in the temperature range of 400–700 °C.

2.2. Characterization

Microscopic investigations were carried out with the help of a high-resolution low-voltage field emission gun scanning electron microscope (SEM, Leo DSM 982 Gemini) and a field emission gun transmission electron microscope (TEM, Philips CM200 FEG). Elemental mapping was performed using energy-dispersive x-ray (EDX) spectroscopy (Noran Pioneer Pulstar Si(Li) x-ray detector). The images were recorded in digital form using 512×512 pixel resolution (at a magnification of 10 000 this refers to 18.3 nm pixel size). EDX mapping was performed using 128×128 pixel resolution at 20 000 magnification (pixel size 36.6 nm).

X-ray powder diffraction (XRD) data were collected on a D8 Advance Bruker diffractometer by using Cu Kα (40 kV, 40 mA) radiation. Raman spectra were recorded using a frequency-doubled Nd:YAG green laser (532.25 nm, 30 mW) and CCD detector. Raman experiments were performed in ambient atmosphere and at room temperature.

Thermogravimetric investigations of pristine cement, activated carbon and CNT-modified cement particle samples were carried out with a Netzsch STA 449 C thermobalance. The samples were slightly ground prior to the measurements. A sample of 9–18 mg was heated
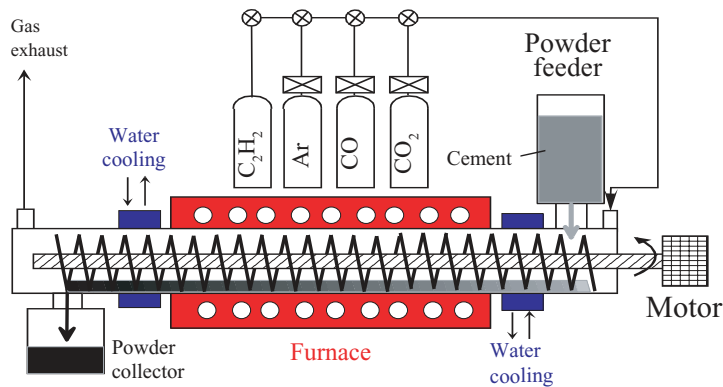
Figure 1. Schematic representation of the experimental setup based on continuous feeding of cement particles using a screw feeder.
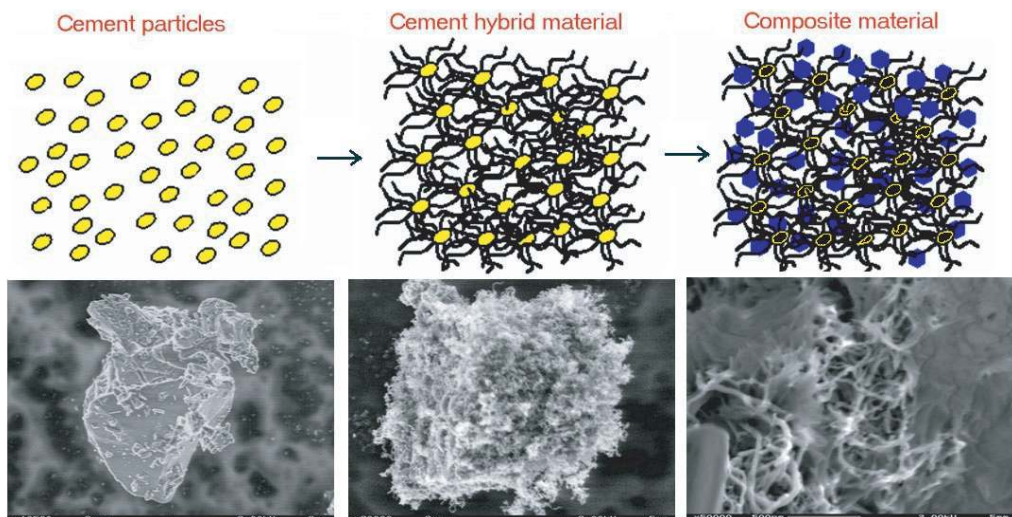
Figure 2. Schematic representation of the general concept of the incorporation of CNTs/CNFs into composite material by their direct growth on the surface of matrix particles.

in an Al_2O_3 crucible from room temperature to $750\,^\circ\text{C}$ with a heating rate of $10\,^\circ\text{C}\,\text{min}^{-1}$ in a dynamic air ($40\,\text{ml}\,\text{min}^{-1}$) atmosphere.

3. Experimental results and discussions

It was found that the product composition can be varied from no carbon precipitated on particles (below $450\,^\circ\text{C}$) to complete coverage of cement particles (figure 2) at higher temperatures. These structures provided a good dispersion of the CNTs and CNFs in the cement matrix, which is essential for the creation of very strong and electrically conductive materials. TEM images show that we have synthesized a cement-based hybrid material consisting of CNTs and CNFs attached to cement particles (figure 3).

Figure 3. TEM images of CHM structures (a) showing complete coverage of the cement particles by carbon material; (b) and (c) revealing the formation of multiwalled CNTs and CNFs.

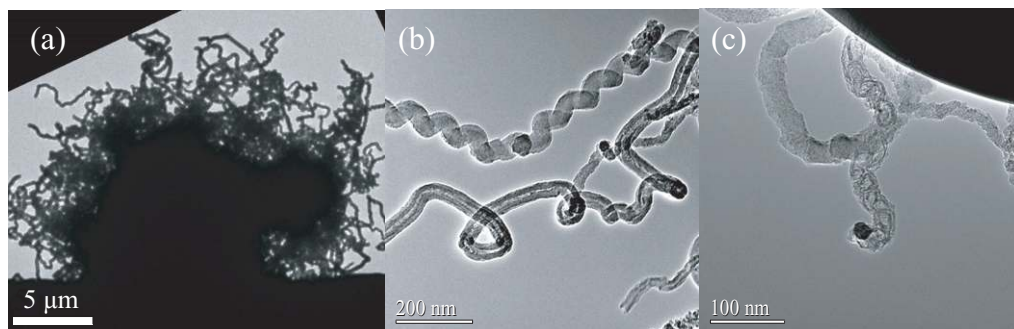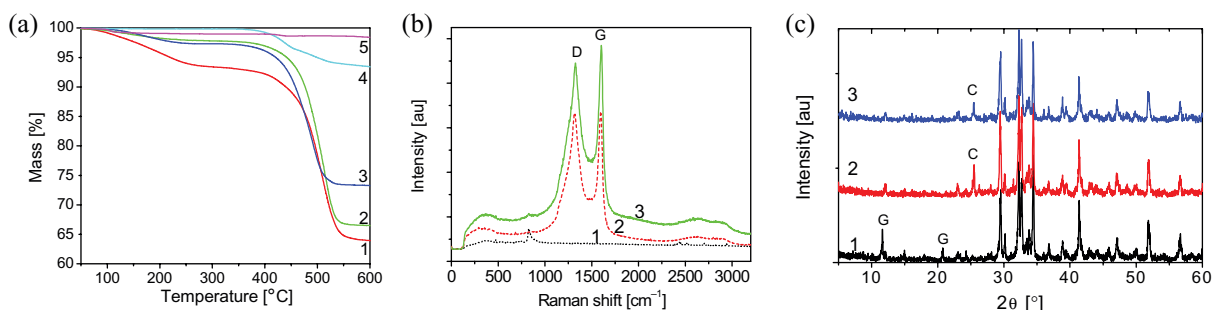**Figure 4.** (a) TGA curves of CHM produced (1) at $600\,^\circ$C and (2) at $550\,^\circ$C under $C_2H_2 + CO$ ($860 + 50\,cm^3\,min^{-1}$), (3) at $525\,^\circ$C under $C_2H_2 + CO$ ($660 + 50\,cm^3\,min^{-1}$), and (4) at $525\,^\circ$C under $C_2H_2 + CO_2$ ($660 + 600\,cm^3\,min^{-1}$) and (5) pristine SR cement. (b) Raman spectra of (1) pristine SR cement and CHM produced from (2) SR and (3) white cements at $550\,^\circ$C under $C_2H_2 + CO$ ($860 + 50\,cm^3\,min^{-1}$). (c) XRD spectra of (1) pristine SR cement and CHM produced (2) at $500\,^\circ$C in $C_2H_2 + CO_2$ ($500 + 500\,cm^3\,min^{-1}$), (3) at $575\,^\circ$C under $C_2H_2 + CO_2$ ($660 + 60\,cm^3\,min^{-1}$) reveal the gypsum (G) decomposition under thermal treatment and appearance of the graphite (C).

The yield of CNTs and CNFs can be easily estimated on the basis of the change of the cement colour from light-brown to black. In order to quantitatively determine the carbon nanomaterial yield, we carried out thermogravimetric analyses (TGA). TGA revealed two features in the temperature ranges 80–280 and 380–560 °C for SR CHM (figure 4(a)). The low-temperature mass decrease can be attributed to hydrocarbons, which were likely formed owing to acetylene polymerization reactions [18]. However the second step can be explained by burning out carbon from the CNTs and CNFs in air atmosphere. The effect of the experimental conditions on the product yields calculated based on the TGA results per mass of raw cement (Y_{cem}) or iron (Y_{Fe}) contained in the cement can be seen from table 2. The most reactive system resulting in the highest carbon yield of $Y_{Fe} = 1660\,\%$ corresponding to $15\,g\,h^{-1}$ was found to be a mixture of acetylene and CO. Interestingly, addition of CO_2 to acetylene did not lead to an increase of the CNT/CNF yield as would have been expected from the literature [19, 20], but as will be shown later it improved the properties of the cement paste. CO alone,

Table 2. Effect of experimental conditions on the product yield obtained on the basis of TGA data and calculated per mass of cement (Y_{cem}) or iron (Y_{Fe}).

T ($^\circ$C)	C_2H_2 (cm^3 min^{-1})	CO_2 (cm^3 min^{-1})	CO (cm^3 min^{-1})	Y_{cem} (%)	Y_{Fe} (%)
525	660	660	0	6.6	240
525	660	660	50	4.9	180
525	0	0	50	0	0
525	660	0	50	33	1150
550	860	0	50	46	1660
550	860	0	177	37	1330
600	860	0	50	45	1610
550[a]	860	0	50	3.3	1430

[a]White cement.

known to be a good carbon precursor for single-walled CNT production [21]–[24], did not form any carbon product under these conditions. Nevertheless, the important role of CO can be attributed to the reduction of iron oxide [25]. Even though the absolute yield of carbon nanomaterials was significantly higher for SR cement, the yield calculated per mass of available iron was found to be very similar for SR and white cements.

Raman experiments performed at ambient atmosphere and temperature showed two main features in the spectra: a G band at about 1600 cm^{-1} and a D band at 1325 cm^{-1} (figure 4(b)). These are typical spectra which can be obtained from multiwalled CNTs [26]. It is worth noting that the results of the Raman measurements did not significantly change when the type of cement or experimental conditions were varied.

In order to examine possible changes in the cement particles under the CHM synthesis conditions, we carried out XRD measurements. No major changes were found in the crystallinity, but a new peak corresponding to graphitized carbon appeared, and the gypsum phase vanished (figure 4(c)). The latter can be explained by the gradual two-stage dehydration process of gypsum (CaSO$_4$·2H$_2$O) in the temperature ranges 120–180 and 180–230 $^\circ$C with the final formation of a crystalline anhydrite (CaSO$_4$) phase at about 450 $^\circ$C [27]. The intensity of other peaks corresponding to different crystalline cement compounds such as Ca$_3$SiO$_5$, Ca$_2$SiO$_4$ and Ca$_3$Al$_2$O$_6$ did not essentially change under the synthesis conditions.

In order to investigate the produced hybrid structures in the quality of a building component, we prepared cement pastes on the basis of CHM and tested their compressive and flexural strengths and electrical resistance. For the current investigations we used beams with dimensions of $60 \times 10 \times 10$ mm^3 prepared using Teflon moulds and cured in water at 20 $^\circ$C for 7, 14 and 28 days. Each series consisted of three beams. The cement paste specimens produced from a mixture of pristine SR cement and SR CHM contained a polycarboxylate-based surfactant available under the commercial name Kolloment (Grace Chemicals), whereas the cement paste specimens produced entirely from SR CHM contained a mixture of two surfactants: Kolloment and Parmix (Finnsementti Oy). The electrical resistance of the cement paste samples was measured using two contacts pressed to opposite sides of the sample through soft graphite films with an area of S separated by a distance of L. The resistivity was determined as $\rho = R \cdot S/L$.

Table 3. Properties of cement paste (7 days curing in water) prepared by adding different samples of SR CHM prepared at a screw feeder rotation rate of $2\,min^{-1}$.

Fraction of CHM (%)	Synthesis conditions			Compressive strength (Mpa)	Flexural strength (Mpa)	Electrical resistivity ($M\Omega\,cm$)	
	Temperature ($^\circ C$)	Gas flow rate ($cm^3\,min^{-1}$)				1 day after	2 months after
		C_2H_2	CO_2				
0	–	–	–	49	16	3.8	9.7
5	600	280	280	38	15	3.1	7.2
10	600	280	280	36	12	2.8	5.9
30	600	280	280	24	8.0	1.7	2.5

The mechanical tests after 7 days curing in water showed that the paste prepared with the addition of CHM is weaker compared with pastes produced from only the pristine SR cement (table 3). Similar results were obtained after curing in water for 14 days. This might be explained by a lower degree of hydration of the modified cement. Comparison of cement paste specimens prepared from pristine SR cement and from the SR CHM produced at $550\,^\circ C$ (under C_2H_2 and CO conditions, i.e. at the highest yield) showed 2.5 times decrease in the compressive and flexural strengths and 70 times increase in the electrical conductivity after 2 months (table 3). It is interesting to note that after drying for 2 months at ambient conditions the most significant decrease in the electrical conductivity of the pastes was observed for samples made of the highest amount of the pristine cement, whereas no time effect was found for samples when 100% CHM samples were used.

The cement pastes made of CHM samples produced at different conditions revealed significant improvement of both mechanical and electrical properties after curing in water for 28 days. As one can see from table 4, the SR CHM can be used to prepare mechanically very strong paste with compressive strength more than 2 times higher than that of paste prepared from the pristine cement. In addition, a paste with up to 40 times better electrical conductivity whilst preserving its mechanical properties can be produced on the basis of our material. To the best of our knowledge, these significant compressive strength and electrical conductivity enhancements are the highest reported so far obtained with the help of CNTs. Up to now, CNTs and CNFs added to cement matrix resulted in either a decrease or a rather small (up to 20%) increase of the compressive strength [28]–[30]. Their main problem was in obtaining a good dispersion of carbon nanomaterials in a matrix. On the other hand, the weakest point in the composite when carbon nanostructures are applied for advanced materials, is in the interfacial bonding between CNTs and the binder matrix. In order to improve the situation, many researchers [28], [31]–[35] utilized treated CNTs/CNFs, e.g. by using ozone gas or sulphuric or nitric acids leading to the formation of carboxylic groups capable of enhancing the reinforcement efficiency between the hydrated cement and CNTs. From that point of view, for increasing the strength of the hardened paste (or concrete) it is very important to attach or even more important to produce CNTs/CNFs attached to cement particles as we demonstrated in this work. Therefore, carbon nanomaterials are easily and homogeneously dispersed in the cement paste and are intermingled with the hydration products during the hydration process.

Table 4. Mechanical (after 28 days curing in water) and electrical (1 day after mechanical testing) properties of cement paste prepared by adding different samples of SR CHM.

Fraction of CHM (%)	Temp (°C)	Gas flow rate ($cm^3 min^{-1}$)			Compressive strength (Mpa)	Electrical resistivity ($M\Omega$ cm)
		C_2H_2	CO_2	CO		
0	—	—	—	—	25	9.7
100	550[a]	860	0	177	22	0.23
100	575[b]	660	660	0	55	1.3
100	500[b]	500	500	0	40	1.7
100	525	660	660	0	56	4.0

[a] $6 min^{-1}$
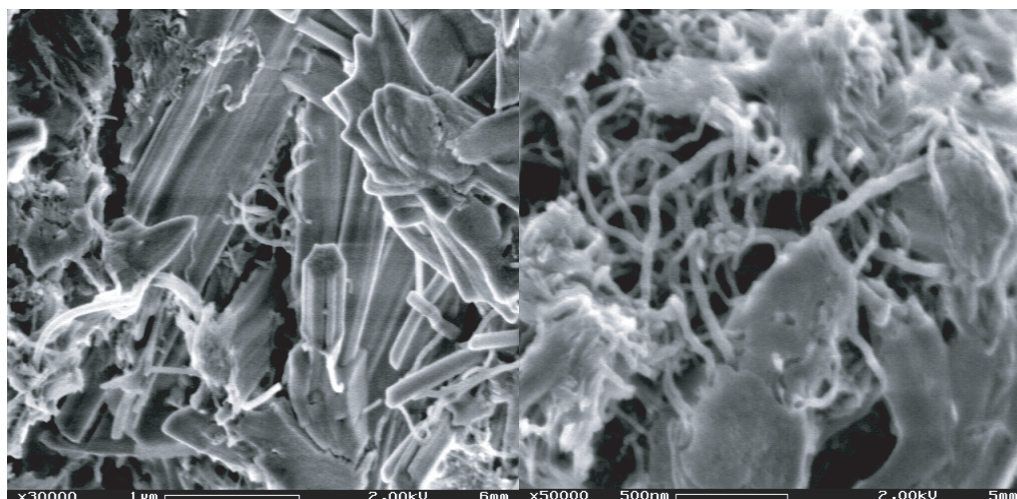[b] $2 min^{-1}$—screw feeder rotation rate.

Figure 5. SEM images of the hardened cement paste (curing in water for 28 days) after the mechanical test. Images revealing the connection formed after the cement hydration process.

It is also important to note that the best mechanical results were obtained from the CHM synthesized in the presence of CO_2, whereas the component needed for the highly conductive paste was fabricated by adding CO in the reactor. If the increase in the electrical conductivity can be explained by higher CNT and CNF yield in the presence of carbon monoxide, the role of CO_2 might be attributed to the etching of amorphous carbon and hydrocarbons formed due to C_2H_2 polymerization.

We have observed the fractured parts of the hydrated (curing in water for 28 days) cement paste specimens by SEM. It was found that the CNTs and CNFs originally attached to the cement particles appeared to be nicely imbedded into the hydration products of the C–S–H phase (figure 5). CNTs and CNFs bridged the neighbouring cement particles surrounded by their hydration products. This could explain the significant increase in the mechanical strength
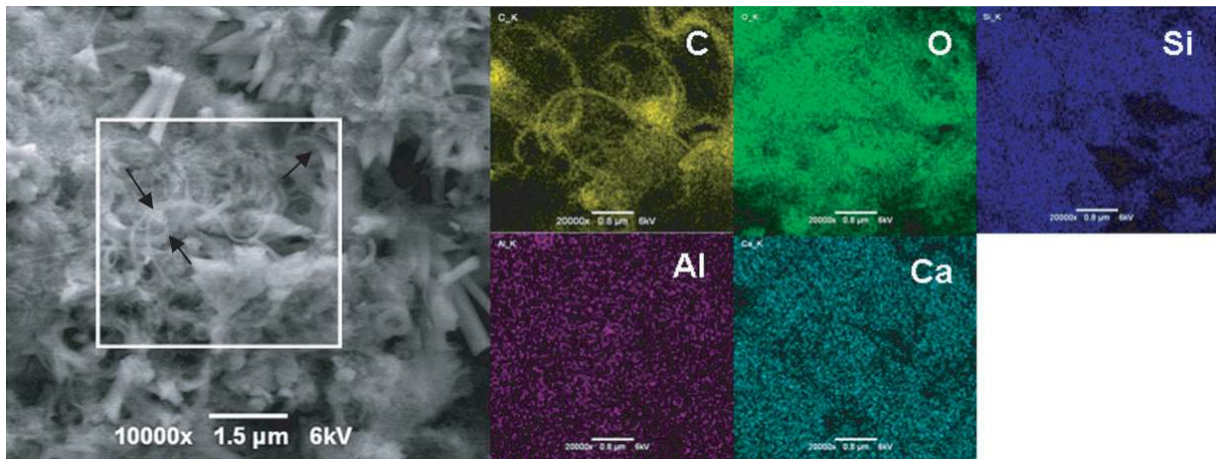
Figure 6. The results of SEM/EDX investigations of the hardened cement paste (curing in water for 28 days) after the mechanical test. The images reveal the presence of carbon nanomaterials (indicated by arrows) and cement composition elements: O, Al, Si and Ca.

and electrical conductivity of the hardened past compared with the paste prepared from the pristine cement. In order to visualize the fracture surface of the hardened paste, we carried out elemental mapping using EDX spectroscopy. The applied electron energy was 6 kV, which allows us to detect all the interesting elements (C, O, Al, Si and Ca) with reasonable count rate. No conductive coating was applied to the analysed sample. In figure 6, the results of the mapping of different elements in the sample collected using net region of interest (ROI) counts for C, O, Al, Si and Ca Kα lines are shown. One can easily distinguish the carbon nanomaterials and cement composition atoms confirming a good dispersion of the CNTs in cement hydration products.

Significant enhancement of the mechanical properties of the SR CHM paste after prolonged water curing was certainly caused by progressing hydration processes. The obtained results also indicate a significantly slower hydration rate of the CHM in comparison with the pristine cement. The difference between the strength properties of CHM and pristine cements can be partially explained by the change of gypsum to its anhydrite form. $CaSO_4$ has a slower dissolution rate compared to gypsum and thereby could be lacking in pore water to hinder the reaction of the $Ca_3Al_2O_6$ clinker phase in the early stages of cement hydration. Also, $CaSO_4$ in cement reacts with batch water and transforms into hemi-hydrate/gypsum, and the water volume available for hydration of calcium silicate hydrate, which is responsible for the good strength properties of concrete, is decreased [27]. This could additionally contribute to the stiffening of the paste in CHM hydration.

4. Conclusion

For the first time, cement particles were utilized both as catalyst and as support material, which allowed us to synthesize novel hybrid nanostructured materials, wherein CNTs and CNFs attached to cement particles and provided a very good dispersion of the carbon nanomaterials

IOP Institute of Physics ⓓ DEUTSCHE PHYSIKALISCHE GESELLSCHAFT

in the cement matrix. This hybrid material was synthesized by a simple one-step CVD method, which can be easily combined into industrial cement production without a significant increase in cement cost. Our investigations based on TEM, SEM, XRD, TGA and Raman measurements showed high efficiency of the method for the low-temperature and high-yield synthesis of CNTs and CNFs. Investigations of the physical properties of the paste made of the CHM revealed as high as a 2 times increase in the compressive strength and a 40 times increase in the electrical conductivity after 28 days curing in water.

Acknowledgments

References

[1] Dresselhaus M S, Dresselhaus G and Eklund P C 1996 *Science of Fullerenes and Nanotubes* (San Diego: Academic)
[2] Reich S, Thomsen C and Maultzsch J 2004 *Carbon Nanotubes* (Weinheim: Wiley-VCH)
[3] Riggs J E, Guo Z X, Carroll D L and Sun Y P 2000 *J. Am. Chem. Soc.* **122** 5879
[4] Zhang X *et al* 2007 *Adv. Mater.* **19** 4198
[5] Calvert P 1999 *Nature* **399** 210
[6] Oncel C and Yurum Y 2006 *Fuller. Nanotub. Carbon Nanostruct.* **14** 17
[7] Saito T, Ohshima S, Xu W C, Ago H, Yumura M and Iijima S 2005 *J. Phys. Chem.* B **109** 10647
[8] Moisala A, Nasibulin A G and Kauppinen E I 2003 *J. Phys.: Condens. Matter* **15** 3011
[9] Nikolaev P, Bronikovski M J, Bradley R K, Rohmund F, Colbert D T, Smith K A and Smalley R E 1999 *Chem. Phys. Lett.* **313** 91
[10] Hata K, Futaba D N, Mizuno K, Namai T, Yumura M and Iijima S 2004 *Science* **306** 1362
[11] Bachilo S M, Balzano L, Herrera J E, Pompeo F, Resasco D E and Weisman R B 2003 *J. Am. Chem. Soc.* **125** 11186
[12] Lolli G, Zhang L, Balzano L, Sakulchaicharoen N, Tan Y and Resasco D E 2006 *J. Phys. Chem.* B **110** 2108
[13] Maruyama S, Kojima R, Miyauchi Y, Chiashi S and Kohno M 2002 *Chem. Phys. Lett.* **360** 229
[14] Harutyunyan A R, Pradhan B K, Kim U J, Chen G and Eklund P C 2002 *Nano Lett.* **2** 525
[15] Pan Z W, Xie S S, Chang B H, Sun L F, Zhou W Y and Wang G 1999 *Chem. Phys. Lett.* **299** 97
[16] Chen P, Zhang H B, Lin G D, Hong Q and Tsai K R 1997 *Carbon* **35** 1495
[17] Bae E J, Choi W B, Jeong K S, Chu J U, Park G S, Song S and Yoo I K 2002 *Adv. Mater.* **14** 277
[18] Ivin K J and Mol J C 1997 *Olefin Metathesis and Metathesis Polymerization* 2nd edn (San Diego: Academic)
[19] Magrez A, Seo J W, Kuznetsov V L and Forro L 2006 *Angew. Chem. Int. Ed. Engl.* **46** 441
[20] Nasibulin A G, Brown D P, Queipo P, Gonzalez D, Jiang H and Kauppinen E I 2006 *Chem. Phys. Lett.* **417** 179
[21] Dai H, Rinzler A, Nikolaev P, Thess A, Colbert D and Smalley R E 1996 *Chem. Phys. Lett.* **260** 471
[22] Pinheiro P, Schouler M C, Gadelle P, Mermouxb M and Dooryhee E 2000 *Carbon* **38** 1469
[23] Queipo P, Nasibulin A G, Jiang H, Gonzalez D, Tapper U, Tsuneta T, Grigoras K, Duenas J A and Kauppinen E I 2006 *Carbon* **44** 1604
[24] Nasibulin A G *et al* 2007 *Nat. Nanotechnol.* **2** 156
[25] Mondal K, Lorethova H, Hippo E, Wiltowski T and Lalvani S B 2004 *Fuel Process. Technol.* **86** 33
[26] Boskovic B O, Stolojan V, Khan R U A, Haq S and Silva S R P 2002 *Nat. Mater.* **1** 165

[27] Sener S, Bilgen S and Ozbayoglu G 2004 *Miner. Eng.* **17** 473
[28] Li G Y, Wang P M and Zhao X 2007 *Cem. Concr. Compos.* **29** 377
[29] Kowlad T 2004 *Proc. Int. Symp. on Ultra High Performance Concrete (Kassel, Germany)* p 195
[30] Makar J M and Beaudoin J J 2003 *Proc. 1st Int. Symp. on Nanotechnology in Construction (Paisley, Scotland)* p 246
[31] Fu X and Chung D D L 1998 *Carbon* **36** 459
[32] Bae J, Jang J and Yoon S H 2002 *Macromol. Chem. Phys.* **203** 2196
[33] Eitan A, Jiang K, Dukes D, Andrews R and Schadler L S 2003 *Chem. Mater.* **15** 3198
[34] Li G Y, Wang P M and Zhao X 2005 *Carbon* **43** 1239
[35] Fu X and Chung D D L 1996 *Cem. Concr. Res.* **26** 1467